Precision evaluation of the ^{71}Ga(ν_e,e^-) solar neutrino capture rate from the (^{3}He,t) charge-exchange reaction

D. Frekers,[1] T. Adachi,[2] H. Akimune,[3] M. Alanssari,[1] B. A. Brown,[4] B. T. Cleveland,[5,*] H. Ejiri,[2] H. Fujita,[2] Y. Fujita,[2,6] M. Fujiwara,[2] V. N. Gavrin,[7] M. N. Harakeh,[8,9] K. Hatanaka,[2] M. Holl,[1] C. Iwamoto,[2] A. Lennarz,[1] A. Okamoto,[2] H. Okamura,[2,†] T. Suzuki,[2] and A. Tamii[2]

[1]*Institut für Kernphysik, Westfälische Wilhelms-Universität Münster, D-48149 Münster, Germany*
[2]*Research Center for Nuclear Physics, Osaka University, Ibaraki, Osaka 567-0047, Japan*
[3]*Department of Physics, Konan University, Kobe 658-8501, Japan*
[4]*National Superconducting Cyclotron Laboratory, The Joint Institute for Nuclear Astrophysics and the Department of Physics and Astronomy, Michigan State University, East Lansing, Michigan 48824, USA*
[5]*Department of Physics, University of Washington, Seattle WA98195, USA*
[6]*Department of Physics, Osaka University, Toyonaka, Osaka 560-0043, Japan*
[7]*Institute for Nuclear Research, Russian Academy of Sciences, Moscow, 117312, Russia*
[8]*Kernfysisch Versneller Instituut, University of Groningen, NL-9747 AA Groningen, The Netherlands*
[9]*GSI Helmholtzzentrum für Schwerinonenforschung GmbH, D-64291 Darmstadt, Germany*

(Received 19 January 2015; published 13 March 2015)

A precision measurement of the ^{71}Ga(^{3}He,t)^{71}Ge charge-exchange reaction was performed. By using a rather complete set of theoretical form factors to describe the cross-section angular distributions over a large angular range, the Gamow-Teller strength distribution up to the effective neutron-separation energy in ^{71}Ge was extracted. The data and the analysis constrain the ^{71}Ga(ν_e,e^-) solar neutrino rate in a neutrino nonoscillation scenario. For nonoscillating neutrinos we report a solar neutrino capture rate of $122.4 \pm 3.4(\text{stat}) \pm 1.1(\text{sys})$ SNU, which is lower than the presently accepted value of 132 ± 18 SNU, though not in disagreement given the quoted errors.

DOI: 10.1103/PhysRevC.91.034608 PACS number(s): 21.10.−k, 23.40.Hc, 25.55.Kr, 27.50.+e

I. INTRODUCTION

Neutrino physics experiments are presently governed by the quest for increased precision and driven by the hope to discover unexpected phenomena, which lie outside the Standard Model. Observations of unexpected phenomena have in fact been reported (see, e.g., Refs. [1–6]) and have led to speculations about additional nonstandard neutrinos. However, a consistent picture, which brings the various observations within a common framework, has not yet emerged [7,8]. In parallel, nuclear physics quantities have come under scrutiny to ensure that nuclear physics uncertainties are not the limiting factors for interpreting neutrino experiments and that they can also safely be excluded as the cause of observed anomalies. In this article, the focus is on the nuclear physics input to the GALLEX and SAGE analyses [5,9–11]. Both experiments confirmed the missing solar neutrino flux discovered by the Homestake experiment [12] and reported an oscillation-related suppression of the solar neutrino reaction rate on ^{71}Ga of $67.6^{\pm 4.0(\text{stat.})}_{\pm 3.2(\text{sys.})}$ SNU (GALLEX/GNO) [10] and $65.4^{+3.1}_{-3.0}$ SNU (SAGE) [5], whereas the expected rate in a nonoscillation scenario was about 132 SNU [13]. Further, both collaborations have since performed calibration measurements of their detectors by employing two reactor-produced neutrino sources, i.e., ^{51}Cr and ^{37}Ar, and found a persistent discrepancy at a 2.5σ significance between the expected and measured neutrino capture rate [5]. Triggered by these results, precision measurements of the ^{71}Ga(ν_e,e^-) cross section using the (^{3}He,t) charge-exchange reaction [14], as well as remeasurements of the Q values for the ^{71}Ga(ν_e,e^-)^{71}Ge reaction and for the ^{51}Cr(EC,ν_e)^{51}V decay, have recently been performed [15,16]. These have ruled out incorrect nuclear physics assumptions as the source of the observed discrepancies.

The present work follows the spirit of Ref. [14] by providing further precision input to solar neutrino properties and solar neutrino matter effects, which are the issues SAGE and GALLEX had focused on. Whereas in Ref. [14] emphasis was on accurate extraction of Gamow-Teller (GT) strength from the ^{71}Ga(^{3}He,t)^{71}Ge reaction to the three lowest-lying states accessible to the ^{51}Cr calibration neutrinos, i.e., the $J^\pi = 1/2^-$ ground state (g.s.), the 175-keV($5/2^-$) state, and the 500 keV($3/2^-$) state, we present here the entire GT-strength distribution up to an effective neutron-separation energy of 8.46 MeV [17]. This allows for an accurate evaluation of the ^{71}Ga(ν_e,e^-) response to the full solar neutrino spectrum seen by the SAGE and GALLEX detectors.

II. EXPERIMENT

The ^{71}Ga(^{3}He,t)^{71}Ge charge-exchange experiment was carried out at the Research Center for Nuclear Physics (RCNP) in Osaka. A 420-MeV ^{3}He^{++} beam was accelerated using the azimuthally varying field cyclotron in combination with the ring cyclotron and transported through the WS beam line [18] to the scattering chamber of the Grand Raiden spectrometer [19]. Outgoing tritons were momentum analyzed in the Grand Raiden spectrometer within its full acceptance of ± 20 mrad in the horizontal direction and ± 40 mrad in the

*Also at SNOLAB, Lively, Ontario, Canada.
†Deceased.

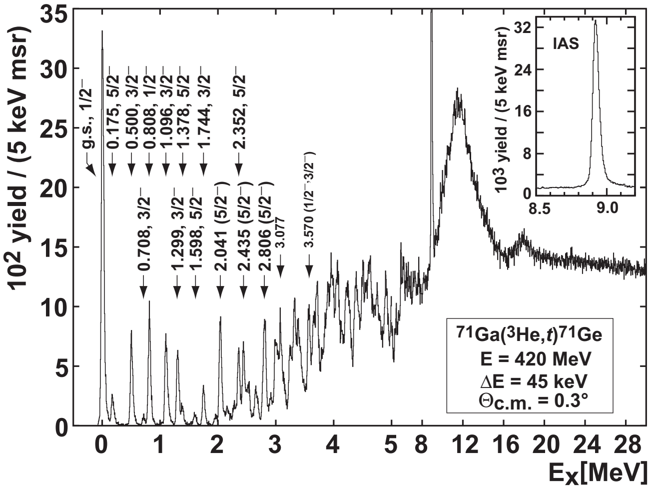

FIG. 1. Excitation-energy spectrum of the ^{71}Ga(^{3}He,t)^{71}Ge reaction at 420 MeV. The inset shows the isobaric analog state resonance at 8.913 MeV. Note the change of the energy scale above 5 MeV. Identified states are given with the assigned spins.

vertical direction. A final spectral energy resolution of 45 keV (full width at half maximum) using the dispersion-matched beam was achieved [20,21]. A full account of the experimental details as well as of the Ga target preparation is given in Refs. [14,22].

A ^{71}Ga(^{3}He,t) excitation spectrum up to 30 MeV is shown in Fig. 1 for a spectrometer-angle setting of zero degree. The most prominent features are the isobaric analog resonance, which appears as a single line at 8.913 MeV, and the Gamow-Teller giant resonance (GTR), which peaks at about 11.75 MeV. The structure at 18.0 MeV is interpreted as the $T_{>}$ component of the GTR [23]. Individual states are identified up to about 3.5 MeV. Spin-parity assignments have been taken from the National Nuclear Data Center data base [24].

III. ANALYSIS

The analysis of the data follows the methods described in Ref. [14] and is summarized only briefly.

In a first step experimental angular distributions were generated for the individual states up to about 3 MeV. These states carry known spins and parities (cf. Fig. 1), and individual B(GT) values were extracted. In a second step, angular distributions were generated for $\Delta E = 0.5$ MeV excitation-energy bins up to an excitation energy of ≈8.5 MeV. This is the effective neutron threshold, because the decay of s-wave neutrons is forbidden [17]. These angular distributions are described separately, and because of unknown spins and parities, a slightly more general set of transition amplitudes is assumed. For the low-energy overlap region between 0 and 3 MeV the two sets allow a consistency check for the B(GT) extraction.

The sets of angular distributions were calculated with the code FOLD [25]. The form factors were generated by double folding the effective nucleon-nucleon interaction of Love and Franey [26,27] at 140 MeV/u over the transition densities of the target-projectile and residue-ejectile systems. One-body transition densities (OBTDs) for the ground state and the three lowest-lying states in ^{71}Ge were calculated with the shell-model code NUSHELLX [28] using the GXPF1a [29,30] interaction in the full fp-model space, and these were taken as

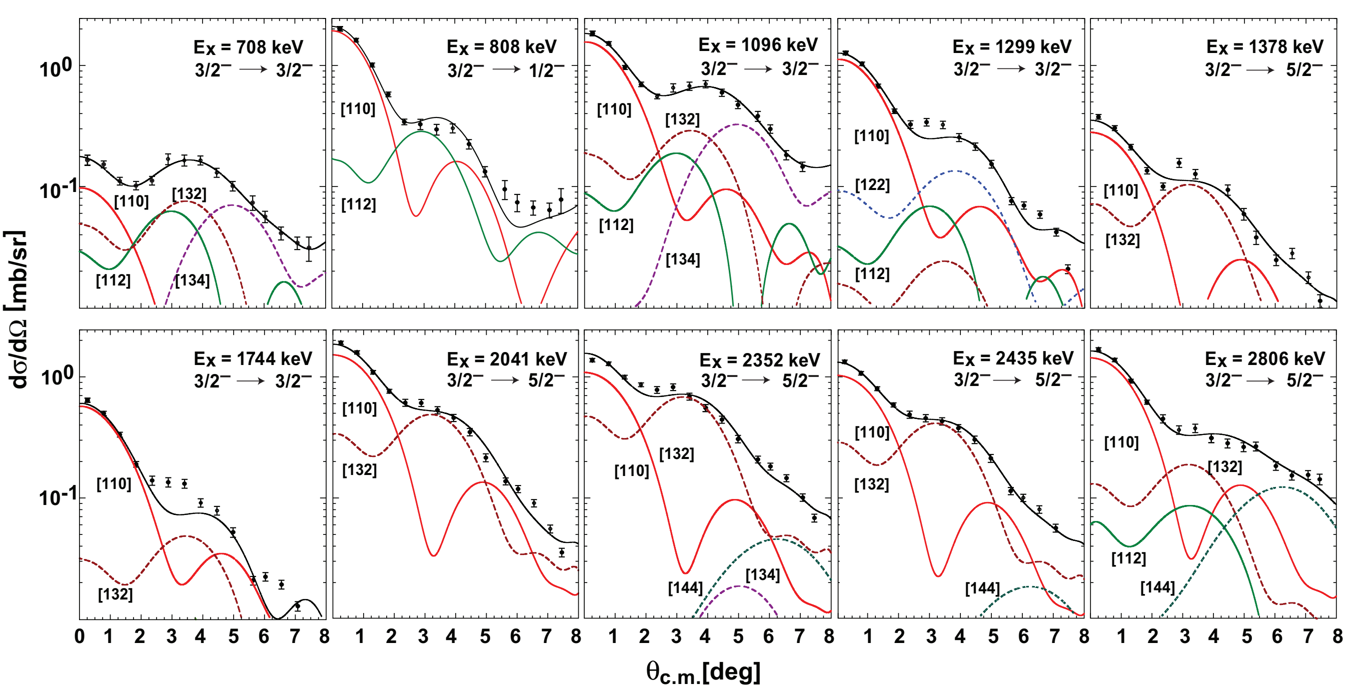

FIG. 2. (Color) Angular distributions for the ^{71}Ga(^{3}He,t) reaction leading to low-lying individual states of known spin and parity in ^{71}Ge. The various curves (color coded) denote the contributions from the different projectile-target angular-momentum-transfer combinations [$J_{\mathrm{proj}} J_{\mathrm{tar}} J_{\mathrm{rel}}$]. The [110] contribution near zero degree is used to extract the strength of the GT transition.

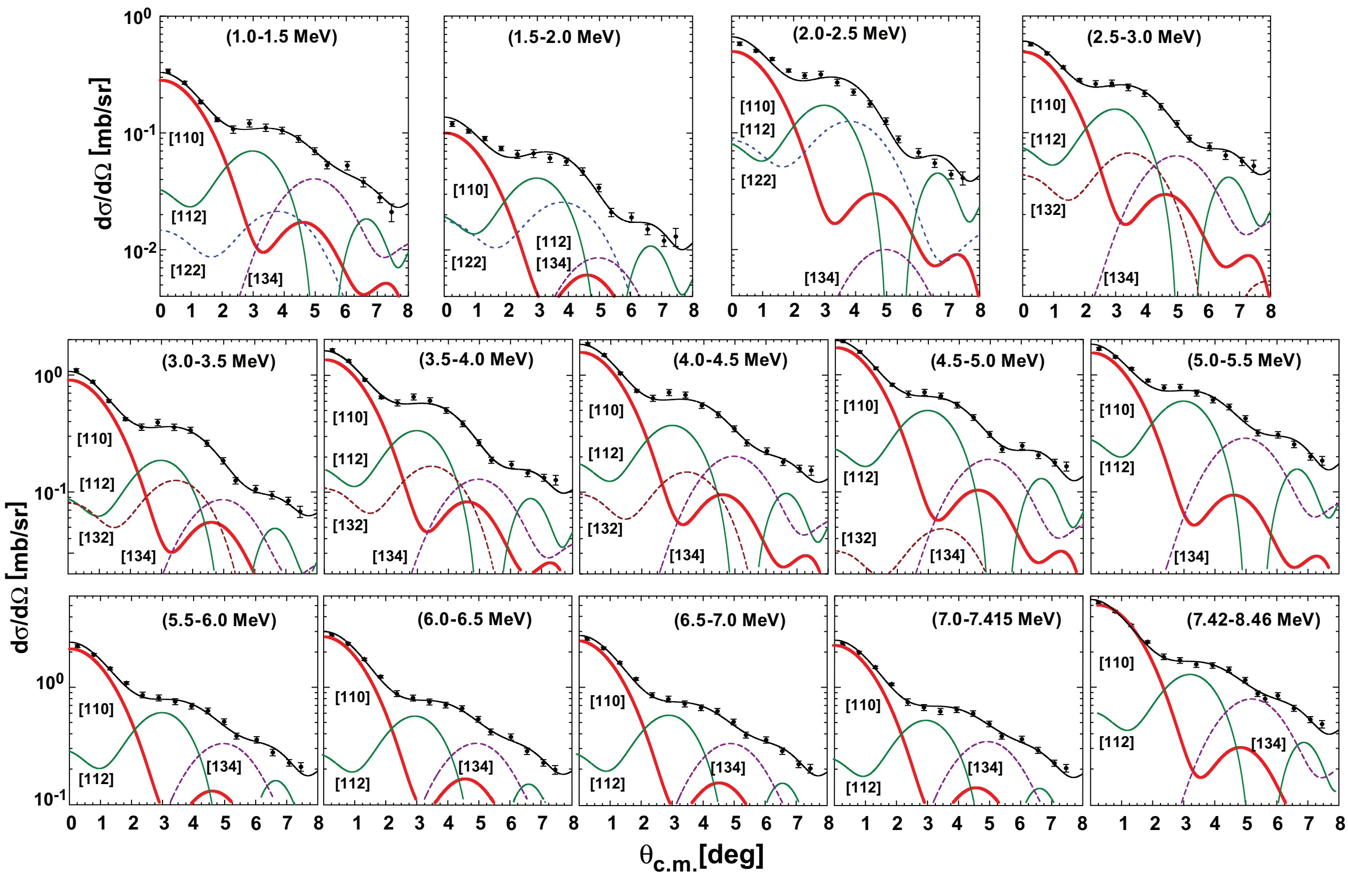

FIG. 3. (Color) Angular distributions for the ^{71}Ga(^{3}He,t) reaction integrated over excitation-energy bins of 500 keV (except for 7.0 and 7.42 MeV). The various curves (color coded) denote the contributions from the different projectile-target angular-momentum-transfer combinations [$J_{\rm proj} J_{\rm tar} J_{\rm rel}$]. The [110] contribution near zero degree is used to extract the GT-transition strength. Note that with increased excitation energy the GT fraction increases owing to the influence of the GTR resonance, which peaks at 11.75 MeV.

a template for the description of all relevant transitions. One can justify this because the B(GT) extraction, which follows from the cross section at momentum transfer $q = 0$, is not sensitive to the details of the underlying nuclear structure. More details can be found in Ref. [14].

The form factors were taken for the possible combinations of target-projectile angular-momentum transfers $\vec{J}_{\rm tar}$, $\vec{J}_{\rm pro}$, and $\vec{J}_{\rm rel} = \vec{J}_{\rm pro} + \vec{J}_{\rm tar}$, which contribute to a transition from the ground state of ^{71}Ga ($J_i = 3/2^-$) to a final state with J_f in ^{71}Ge. In the following, these components are denoted as [$J_{\rm pro}$ $J_{\rm tar}$ $J_{\rm rel}$] (see also Figs. 2 and 3). For the present (^{3}He,t) reaction, $\vec{J}_{\rm rel} = \Delta\vec{L}_{\rm tar}$, which is the orbital angular-momentum transfer to the target system. Therefore, the shapes of the angular distributions are similar for transitions with equal $J_{\rm rel}$. In the present scheme, the [$J_{\rm pro} J_{\rm tar} J_{\rm rel}$] contributions to parity nonchanging transitions of potentially GT type (i.e., $3/2^- \rightarrow 1/2^-, 3/2^-, 5/2^-$) are limited to even values of $J_{\rm rel}$. For transitions from $3/2^- \rightarrow 1/2^-$ possible values for $J_{\rm rel}$ are $J_{\rm rel} = 0$ and 2, whereas for those from $3/2^- \rightarrow 3/2^-, 5/2^-$ possible values for $J_{\rm rel}$ are $J_{\rm rel} = 0, 2$, and 4. We also note that the [110] component with $J_{\rm rel} = 0$ denotes the GT part of the transition.

These form factors then served as input to calculations in a distorted-wave Born approximation (DWBA) (for more information consult Ref. [14]).

The calculated DWBA cross-section angular distributions were used to fit the experimental angular distributions for each transition, whereby the different [$J_{\rm pro} J_{\rm tar} J_{\rm rel}$] sets were varied independently to match the data. The various sets are added incoherently, because they are quantum-mechanically distinguishable. Because the experimental data sets cover a relatively large angular range, the procedure allows isolating the [110] GT part of the cross section at zero degree rather reliably.

Figure 2 shows a representative set of angular distributions for individual states below 3 MeV excitation and with different final-state spins. In all cases the [110] GT part is the dominant component near zero degree, confirming that the extraction of the zero-degree fraction of the GT contribution (and consequently also the fraction of the non-GT contribution) is in fact quite robust. Further, the [110] parts for different final-state spins differ only in the position of the second diffraction maximum, which shifts from $\approx 4^\circ$ to $\approx 5^\circ$, as the final-state spins change from $J^\pi = 1/2^-$ to $J^\pi = 5/2^-$. One may also note that the various [$J_{\rm pro} J_{\rm tar} J_{\rm rel}$] components were determined strictly through a χ^2 minimization, and ambiguities for the components with $J_{\rm rel} \neq 0$, which all peak at similar finite angles, may exist.

The extraction of B(GT) values from the extrapolated $q = 0$ GT cross sections follows the recipe described in

TABLE I. Energy levels, spins, cross sections, B(GT) fractions, and B(GT) values for levels populated via the ^{71}Ga(^{3}He,t)^{71}Ge reaction. Columns one and two: Energy levels and J^π values taken from Ref. [24] (spins quoted if known; errors quoted if significant). Columns three to seven: Excitation energies (errors ± 1 keV) deduced from the present experiment, J^π values taken for the angular-distribution fits, cross sections at $q = 0$, their GT fraction, and B(GT) values. Cross-section errors are statistical. Errors for B(GT) values include an extra 50% contribution from the non-GT part of the cross section at $q = 0$, except for the ground-state (g.s.) transition, where this error (i.e., 4%) enters as a systematic error in the later analysis. The energy regions above 1 and above 2 MeV are separated by extra space. Spin assignments above 2 MeV from the present analysis in brackets are only indicative. They are based on the χ^2 minimization of the angular-distribution fits described in the text.

E_x(^{71}Ge) Ref. [24]		E_x(^{71}Ge)		$\frac{d\sigma}{d\Omega}(q=0)$	GT	B(GT)
keV	J^π	keV	J^π	(mb/sr)	%	$\times 10^{-2}$
0	$\frac{1}{2}^-$	g.s.	$\frac{1}{2}^-$	0.786(9)	92	8.52(11)[a]
174.9	$\frac{5}{2}^-$	175	$\frac{5}{2}^-$	0.071(4)	40	0.34(26)
499.9	$\frac{3}{2}^-$	500	$\frac{3}{2}^-$	0.171(4)	87	1.76(14)
708.2	$\frac{3}{2}^-$	708	$\frac{3}{2}^-$	0.018(1)	55	0.11(5)
808.2	$\frac{1}{2}^-$	808	$\frac{1}{2}^-$	0.210(4)	92	2.29(10)
1095.5	$\frac{3}{2}^-$	1096	$\frac{3}{2}^-$	0.184(4)	84	1.83(17)
1298.7	$\frac{3}{2}^-$	1299	$\frac{3}{2}^-$	0.126(2)	89	1.33(8)
1378.6	$(\frac{3}{2}^+,\frac{5}{2},\frac{7}{2})$	1378	$\frac{5}{2}^-$	0.035(3)	80	0.33(4)
1598.5	$\frac{3}{2}^-$	1598	$\frac{3}{2}^-$	0.018(2)	51	0.11(5)
1743.4	$\frac{3}{2}^-$	1744	$\frac{3}{2}^-$	0.061(1)	94	0.68(2)
1965.0	$\frac{3}{2}^-$	1964	$\frac{3}{2}^-$	0.020(2)	50	0.12(6)
2043(2)	$\frac{1}{2}^-,\frac{3}{2}^-$	2041	$(\frac{3}{2}^-,\frac{5}{2}^-)$	0.187(3)	82	1.81(2)
2146.1	$\frac{1}{2},\frac{3}{2}$	2145	$(\frac{3}{2}^-,\frac{5}{2}^-)$	0.036(1)	72	0.31(6)
2278(3)	$(\frac{5}{2}^+,\frac{1}{2}^-,\frac{3}{2}^-)$	2276	$(\frac{1}{2}^-,\frac{3}{2}^-)$	0.046(1)	66	0.36(9)
2351.5(2)	$\frac{1}{2}^-,\frac{3}{2}^-$	2352	$(\frac{3}{2}^-,\frac{5}{2}^-)$	0.157(2)	70	1.30(28)
2435.2(1)	$\frac{1}{2},\frac{3}{2},\frac{5}{2}^+$	2435	$(\frac{3}{2}^-,\frac{5}{2}^-)$	0.133(2)	78	1.23(17)
2644(3)	$\frac{5}{2}^+$	2642	$(\frac{5}{2}^-)$[b]	0.062(1)	73	0.54(10)
2775(3)	$(\frac{1}{2},\frac{3}{2})$	2778	$(\frac{5}{2}^-)$	0.070(1)	70	0.58(12)
2802(5)		2806	$(\frac{5}{2}^-)$	0.165(3)	88	1.72(12)
2890(3)		2888	$(\frac{5}{2}^-)$	0.028(4)	57	0.19(7)
2922(5)		2924	$(\frac{5}{2}^-)$	0.052(1)	54	0.33(14)

[a]Reference value adjusted to the ft value (cf. [14]); the errors quoted for this value and all other values are of a statistical nature.
[b]Negative parity favored in the present analysis.

Ref. [14]. A list of the relevant extracted quantities is given in Table I.

The calculated DWBA cross sections for the $\Delta E = 0.5$ MeV energy bins are presented in Fig. 3. In these cases the calculations to fit the experimental data were performed throughout for a final-state spin of $3/2^-$, which was motivated by the lowest χ^2 values. The procedure receives some justification, because the extraction of the B(GT) strength for each energy bin is to a large extent independent of the final-state spin assumption. Further, because the OBTDs were generated in the restricted fp-model space, form factors with odd $J_{\rm rel}$, which lead to positive-parity final states are not included in these calculations. This may have an effect on the angular distribution fits at finite momentum transfer, but since the odd $J_{\rm rel}$ angular distributions fall off steeply towards zero degree and the transition strengths to known states are found to be comparatively weak, the present procedure of extracting the B(GT) strength remains unaffected. A consistency check was performed for the low-energy region, where the results from this procedure were compared with those from the analysis of the individual states described before. The integrated strength for each energy bin as well as the summed strength for the individual states up to 3 MeV yielded almost identical results (cf. Table II). As further indicated in Table II, the total integrated B(GT) strength up to the effective neutron-decay threshold at 8.46 MeV is $B(\mathrm{GT}) = 3.01(7)$. This integrated value is lower by nearly 25% compared to earlier (^{3}He,t) measurements reported in Ref. [17], which is attributed to the different analysis performed in Ref. [17], in which the non-GT part of the zero-degree cross section could not be as accurately determined. The effect on the solar neutrino capture rate is, however, much less pronounced, as shown below.

TABLE II. B(GT)-strength values extracted from 0.5-MeV energy bins and compared with those of individual states summed over the same energy bin.

^{71}Ge E_x (MeV)	GT %	B(GT) $\Delta E = 0.5$ MeV	B(GT) Indiv. states
0.0–0.5	90	0.088(5)[a]	0.106(8)
0.5–1.0	85	0.029(3)	0.024(2)
1.0–1.5	86	0.034(3)	0.035(3)
1.5–2.0	73	0.012(2)	0.009(1)
2.0–2.5	75	0.060(10)	0.055(11)
2.5–3.0	80	0.059(7)	0.035(6)
3.0–3.5	84	0.110(10)	–
3.5–4.0	84	0.165(16)	–
4.0–4.5	85	0.191(17)	–
4.5–5.0	87	0.209(16)	–
5.0–5.5	84	0.191(18)	–
5.5–6.0	88	0.265(19)	–
6.0–6.5	90	0.338(18)	–
6.5–7.0	90	0.315(17)	–
7.0–7.42	90	0.289(16)	–
7.42–8.46	89	0.645(39)	–
	$\sum_{0-3\mathrm{MeV}}$	=0.281(14)	$\sum_{0-3\mathrm{MeV}} = 0.265(15)$
	$\sum_{\mathrm{total}}$	=3.01(7)	

[a]The B(GT) of the state at 499.9 keV has been divided into two bins.

IV. SOLAR NEUTRINO CAPTURE RATES

Table III lists solar neutrino capture rates as a function of the excitation energy in ^{71}Ge using the B(GT) values given in Table I (up to 3 MeV) and Table II (3 MeV and above). The cross-section calculations were made using the program

TABLE III. Solar neutrino capture rates as a function of excitation energy in ^{71}Ge calculated from the B(GT) values listed in Table I. Above $E_x = 3$ MeV the rates are evaluated for ± 0.25-MeV energy bins. Above 7 MeV the energy bin is reduced to ± 0.21 MeV, in order to properly extend to the neutron-separation energy at $S_n = 7.416$ MeV (also cf. Figs. 2 and 3). A capture rate of 0.32 SNU was evaluated for excitation energies above the neutron threshold, $E_x > S_n$ [17]. Errors are statistical errors from the present measurements.

E_x	SNU	E_x	SNU	E_x	SNU	E_x	SNU
0	109.8(13)	1.599	0.013(6)	2.644	0.046(9)	4.75	0.82(7)
0.175	1.2(7)	1.743	0.077(3)	2.775	0.048(10)	5.25	0.61(6)
0.500	2.7(2)	1.965	0.013(6)	2.802	0.140(11)	5.75	0.67(5)
0.708	0.03(1)	2.043	0.187(6)	2.890	0.015(6)	6.25	0.66(4)
0.808	0.61(7)	2.146	0.031(6)	2.922	0.026(11)	6.75	0.47(3)
1.095	0.33(3)	2.278	0.035(9)	3.25	0.77(7)	7.21	0.33(2)
1.299	0.17(1)	2.351	0.12(3)	3.75	0.96(10)	$>S_n$	0.32(2)
1.379	0.041(5)	2.435	0.11(2)	4.25	0.92(9)	$\sum$	122.4(16)

SPECCROSS.F written by Bahcall, which contains corrections for (i) forbidden transitions, (ii) overlap between initial and final atomic states, (iii) exchange effects among electrons, (iv) electron screening, and (v) the nuclear size [31,32]. If we use the same B(GT)-strength spectrum as was used by Bahcall, we obtain results identical to those in Ref. [31]. The cumulative capture rates are shown in Fig. 4.

About 90% of the solar neutrino capture rate directly populates the ground state of ^{71}Ge, which is a consequence of its sensitivity to a significant fraction of the *pp* and the ^{7}Be neutrino spectrum [13,31]. This also implies that the error of the ground-state neutrino capture rate enters with a large weight factor into the overall error calculation. In the present case the measured ground-state [110] GT transition strength (cf. Ref. [14]) is therefore normalized to the precisely determined ft value, whose error is evaluated from the recent Q-value measurement to 1% (cf. Ref. [15]). This 1% error enters as a systematic uncertainty on top of the individual errors given in Table I and on top of the final total capture rate. In determining the individual error values appearing in this Table I, we have taken an arbitrary, yet conservative, approach, as described in Ref. [14], i.e., adding for each transition a 50% fraction of the non-GT part of the zero-degree cross section to the statistical error. For example, in Figs. 2 and 3 this fraction constitutes 50% of the difference between the full curves matching the data and the curves labeled as [110] at a scattering angle of $\theta_{\text{c.m.}} = 0^\circ$. Assuming no correlation

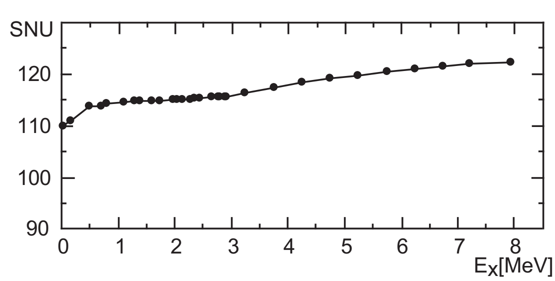

FIG. 4. Cumulative SNU rates as a function of excitation energy in ^{71}Ge.

TABLE IV. Column one: Solar neutrino components. Column two: Cross sections calculated for B(GT) values reported here assuming an oscillation-free neutrino spectrum. Uncertainties are due to uncertainties in B(GT); additional uncertainties [31] are 2.5% for forbidden transitions, 0.4% for electron exchange (*pp* only), and 1.5% for spectrum shape (^{8}B only). Column three: Evaluated solar fluxes from the best fit to all solar neutrino experiments [33], where apart from the *pp* flux, which was constrained by the sun luminosity, the other fluxes were determined from measurements of neutrinos by the Borexino, SNO and Super-Kamiokande experiments. Column four: Neutrino capture rates. The hep contribution of 0.1 SNU is obtained using the upper limit flux estimate of the SNO Collaboration [34]. (Note that Bahcall's estimate lies at 0.01 SNU [35], however, with a nonquantifiable uncertainty.) The uncertainties are evaluated from the solar flux uncertainties (column three), which are quoted in Ref. [33]. The ^{13}N, ^{15}O, and ^{17}F components are combined into a single entry, where the 3σ upper limit quoted in Ref. [33] was converted to 1σ value with a 100% uncertainty. The ^{8}B entry includes 0.3 SNU for capture to levels above the neutron-separation energy [17].

Solar component	Cross section (10^{-46}cm^2)	Solar flux (cm^{-2}sec^{-1})	Capture rate (SNU)
pp	11.60(6)	$6.02^{(1)}_{(6)} \times 10^{10}$	69.9(7)
pep	207(4)	$1.63(34) \times 10^8$	3.4(7)
hep	$588(11)\times 10^2$	$1.2(12) \times 10^4$	0.1(1)
^{7}Be	73.5(15)	$4.99(25) \times 10^9$	36.7(18)
^{8}B	$188(4)\times 10^2$	$5.39(16) \times 10^6$	10.1(3)
^{13}N	61.4(12)		
^{15}O	115(24)	$< 2.3(23) \times 10^8$	2.2(22)
^{17}F	115(24)		
			$\sum = 122.4(30)$

between the various transitions, one can add these extra contributions in quadrature to the statistical errors, which are the ones appearing in Tables I–III. The ground-state transition, however, needs to be treated differently. Here the uncertainty of the non-GT part of the charge-exchange cross section (i.e., 4%) enters as a systematic uncertainty for the transitions to the excited states.

In Table IV we give cross sections for the various components of the solar neutrino spectrum. Comparing the cross sections calculated here to those in Ref. [31], we note that the new B(GT) values result in an increase in the cross section for the medium-energy flux components (pep, ^{7}Be, and CNO) and a decrease in the cross section for the higher-energy components (^{8}B and hep). Also given in Table IV are the solar fluxes for each solar neutrino component together with the capture rates in ^{71}Ga assuming a nonoscillation scenario. The individual fluxes and uncertainties were derived from a fit to the results of all solar neutrino experiments [33]. We note that in these calculations the neutrino flux from the CNO cycle is the biggest contributor to the total error value.

From Tables III and IV the total solar neutrino capture rate on ^{71}Ga is evaluated as

$$R_\odot = 122.4 \pm 1.6(\text{stat}) \pm 3.0(\text{stat}) \pm 0.5(\text{sys}) \pm 1.0(\text{sys})\,\text{SNU},$$

where the first error denotes the statistical error from the present measurements, the second is mostly the result of the uncertainty in the calculated total solar flux, the third is due to the uncertainty in the $B(\mathrm{GT})$ extraction from the $^{71}\mathrm{Ga}(^3\mathrm{He},t)$ transition to the ground state of $^{71}\mathrm{Ge}$ (which is 4% to the sum of the capture rates to the excited states), and the fourth is due to the uncertainty of the ground-state ft value. Errors one and two, as well as errors three and four can be added in quadrature, which yields

$$R_\odot = 122.4 \pm 3.4(\mathrm{stat}) \pm 1.1(\mathrm{sys})\mathrm{SNU}.$$

V. CONCLUSION

We have presented precision data for the solar neutrino capture rate on $^{71}\mathrm{Ga}$. These have been deduced from a $(^3\mathrm{He},t)$ charge-exchange experiment on $^{71}\mathrm{Ga}$ at an incident energy of 420 MeV and with a final-state energy resolution of 45 keV. An elaborate analysis based on theoretical form factors and one-body transition densities from the shell-model code NUSHELLX using the GXPF1a interaction in the full fp-model space, allowed extracting reliable GT cross sections near zero degree, where theoretical uncertainties are comparatively small. Absolute $B(\mathrm{GT})$ values have been evaluated from these cross sections, from which neutrino capture rates for solar neutrinos were calculated. We report a total neutrino capture rate of $122.4 \pm 3.4(\mathrm{stat}) \pm 1.1(\mathrm{sys})$ SNU for the full solar neutrino spectrum. This value is lower than, though still consistent with, the previously accepted value of 132 ± 18 SNU. With the new $B(\mathrm{GT})$ values, the dominant statistical uncertainty of the $^{71}\mathrm{Ga}$ capture rate is now in the solar fluxes, most notably in those from the CNO cycle.

ACKNOWLEDGMENTS

We thank the RCNP accelerator staff for their fine technical support during the course of the experiment. We would also like to thank N. Aoi, J. Lee, K. Miki, Y. Yasuda, and J. Zenihiro for their effort during the preparation of the experiment and C. Peña-Garay for providing us with John Bahcall's program that calculates the cross section for neutrino capture. We are indebted to W. Haxton for assisting us in calculating the neutrino cross sections. The generous financial support from the Directorate of RCNP is gratefully acknowledged. This work was supported by the Deutsche Forschungsgemeinschaft (Germany) (DFG) under Grant No. FR 601/3-1. M.A. acknowledges the financial support from Al-Nahrain University/Ministry of Higher Education and Scientific Research of Iraq (Republic of Iraq). Y.F. and A.T. were partly supported by MEXT (Japan) under Grant No. 22540310.

[1] A. Aguilar, L. B. Auerbach, R. L. Burman, D. O. Caldwell, E. D. Church, A. K. Cochran, J. B. Donahue, A. Fazely, G. T. Garvey, R. M. Gunasingha *et al.* (LSND Collaboration), Phys. Rev. D **64**, 112007 (2001).

[2] A. A. Aguilar-Arevalo, C. E. Anderson, S. J. Brice, B. C. Brown, L. Bugel, J. M. Conrad, Z. Djurcic, B. T. Fleming, R. Ford, F. G. Garcia *et al.* (MiniBooNE Collaboration), Phys. Rev. Lett. **103**, 111801 (2009).

[3] A. A. Aguilar-Arevalo, C. E. Anderson, S. J. Brice, B. C. Brown, L. Bugel, J. M. Conrad, R. Dharmapalan, Z. Djurcic, B. T. Fleming, R. Ford *et al.* (MiniBooNE Collaboration), Phys. Rev. Lett. **105**, 181801 (2010).

[4] Th. A. Mueller, D. Lhuillier, M. Fallot, A. Letourneau, S. Cormon, M. Fechner, L. Giot, T. Lasserre, J. Martino, G. Mention *et al.*, Phys. Rev. C **83**, 054615 (2011).

[5] J. N. Abdurashitov, V. N. Gavrin, V. V. Gorbachev, P. P. Gurkina, T. V. Ibragimova, A. V. Kalikhov, N. G. Khairnasov, T. V. Knodel, I. N. Mirmov, A. A. Shikhin *et al.*, Phys. Rev. C **80**, 015807 (2009).

[6] V. N. Gavrin, V. V. Gorbachev, E. P. Veretenkin, and B. T. Cleveland, arXiv:1006.2103v2.

[7] J. Kopp, M. Maltoni, and T. Schwetz, Phys. Rev. Lett. **107**, 091801 (2011).

[8] K. N. Abazajian, M. A. Acero, S. K. Agarwalla, A. A. Aguilar-Arevalo, C. H. Albright, S. Antusch, C. A. Arguelles, A. B. Balantekin, G. Barenboim, V. Barger *et al.*, arXiv:1204.5379.

[9] W. Hampel, G. Heusser, J. Kiko, T. Kirsten, M. Laubenstein, E. Pernicka, W. Rau, U. Rönn, C. Schlosser, M. Wójcik *et al.*, Phys. Lett. B **420**, 114 (1998).

[10] F. Kaether, W. Hampel, G. Heusser, J. Kiko, and T. Kirsten, Phys. Lett. B **685**, 47 (2010).

[11] J. N. Abdurashitov, V. N. Gavrin, S. V. Girin, V. V. Gorbachev, T. V. Ibragimova, A. V. Kalikhov, N. G. Khairnasov, T. V. Knodel, V. N. Kornoukhov, I. N. Mirmov *et al.*, Phys. Rev. C **59**, 2246 (1999).

[12] B. T. Cleveland, T. Daily, R. Davis, Jr., J. Distel, K. Lande, C. K. Lee, and P. Wildenhain, Astrophys. J. **496**, 505 (1998).

[13] J. N. Bahcall and M. H. Pinsonneault, Rev. Mod. Phys. **64**, 885 (1992).

[14] D. Frekers, H. Ejiri, H. Akimune, T. Adachi, B. Bilgier, B. A. Brown, B. T. Cleveland, H. Fujita, Y. Fujita, M. Fujiwara *et al.*, Phys. Lett. B **706**, 134 (2011).

[15] D. Frekers, M. C. Simon, C. Andreoiu, J. C. Bale, M. Brodeur, T. Brunner, A. Chaudhuri, U. Chowdhury, J. R. Crespo López-Urrutia, P. Delheij *et al.*, Phys. Lett. B **722**, 233 (2013).

[16] T. D. Macdonald, B. E. Schultz, J. C. Bale, A. Chaudhuri, U. Chowdhury, D. Frekers, A. T. Gallant, A. Grossheim, A. A. Kwiatkowski, A. Lennarz *et al.*, Phys. Rev. C **89**, 044318 (2014).

[17] H. Ejiri, H. Akimune, Y. Arimoto, I. Daito, H. Fujimura, Y. Fujita, M. Fujiwara, K. Fushimi, M. B. Greenfield, M. N. Harakeh *et al.*, Phys. Lett. B **433**, 257 (1998).

[18] T. Wakasa, K. Hatanaka, Y. Fujita, G. P. A. Berg, H. Fujimura, H. Fujita, M. Itoh, J. Kamiya, T. Kawabata, K. Nagayama *et al.*, Nucl. Instrum. Methods Phys. Res., Sect. A **482**, 79 (2002).

[19] M. Fujiwara, H. Akimune, I. Daito, H. Fujimura, Y. Fujita, K. Hatanaka, H. Ikegami, I. Katayama, K. Nagayama, N. Matsuoka *et al.*, Nucl. Instrum. Methods Phys. Res., Sect. A **422**, 484 (1999).

[20] H. Fujita, G. P. A. Berg, Y. Fujita, K. Hatanaka, T. Noro, E. J. Stephenson, C. C. Foster, H. Sakaguchi, M. Itoh, T. Taki *et al.*, Nucl. Instrum. Methods Phys. Res., Sect. A **469**, 55 (2001).

[21] H. Fujita, Y. Fujita, G. P. A. Berg, A. D. Bacher, C. C. Foster, K. Hara, K. Hatanaka, T. Kawabata, T. Noro, H. Sakaguchi

et al., Nucl. Instrum. Methods Phys. Res., Sect. A **484**, 17 (2002).

[22] D. Frekers, A. Lennarz, P. Puppe, and J. H. Thies, Nucl. Instrum. Methods Phys. Res., Sect. A **621**, 704 (2010).

[23] D. E. Bainum, J. Rapaport, C. D. Goodman, D. J. Horen, C. C. Foster, M. B. Greenfield, and C. A. Goulding, Phys. Rev. Lett. **44**, 1751 (1980).

[24] National Nuclear Data Center, Brookhaven National Laboratory (2011), http://www.nndc.bnl.gov.

[25] J. Cookand J. A. Carr, computer program FOLD, Florida State University (unpublished, 1988), based on F. Petrovich and D. Stanley, Nucl. Phys. A **275**, 487 (1977), modified as described in J. Cook, K. W. Kemper, P. V. Drumm, L. K. Fifield, M. A. C. Hotchkis, T. R. Ophel, and C. L. Woods, Phys. Rev. C **30**, 1538 (1984), and R. G. T. Zegers, S. Fracasso and G. Colò, NSCL, Michigan State University (unpublished, 2006).

[26] W. G. Love and M. A. Franey, Phys. Rev. C **24**, 1073 (1981).

[27] M. A. Franey and W. G. Love, Phys. Rev. C **31**, 488 (1985).

[28] B. A. Brownand W. D. M. Rae, Nuclear Data Sheets **120**, 115 (2014).

[29] M. Honma, T. Otsuka, B. A. Brown, and T. Mizusaki, Phys. Rev. C **65**, 061301(R) (2002).

[30] M. Honma, T. Otsuka, B. A. Brown, and T. Mizusaki, Eur. Phys. J. A **25**, 499 (2005).

[31] J. N. Bahcall, Phys. Rev. C **56**, 3391 (1997).

[32] J. N. Bahcall and B. R. Holstein, Phys. Rev. C **33**, 2121 (1986).

[33] A. Ianni, Phys. Dark Universe **4**, 44 (2014).

[34] B. Aharmim, S. N. Ahmed, A. E. Anthony, E. W. Beier, A. Bellerive, M. Bergevin, S. D. Biller, M. G. Boulay, Y. D. Chan, M. Chen *et al.*, Astrophys. J. **653**, 1545 (2006).

[35] J. N. Bahcall and P. I. Krastev, Phys. Lett. B **436**, 243 (1998).